SLAC-PUB-7630
Aug/97

Measurement of A_b from Left-Right Forward-Backward Asymmetry in Z^0 Decays using Charged Kaon Tagging

The SLD Collaboration [1]

Abstract

We present a direct measurement of the parity-violating parameter A_b by analyzing the left-right forward-backward asymmetry of b quarks in polarized Z^0 decays with a final state kaon charge tag. The 1994-1995 SLD data sample of 100,000 hadronic Z^0 decays produced with a highly polarized electron beam is used for this analysis. A b-enriched sample is obtained from a vertex-mass tag using a CCD-based vertex detector. The b quark charge is assigned on the basis of the charge of a kaon from the B decay cascade. The charged kaon is identified by the Cerenkov Ring Imaging Detector. The parameter A_b is extracted by forming a double asymmetry in polarization (left-right) and polar angle (forward-backward), with a preliminary result of $A_b = 0.891 \pm 0.083_{stat} \pm 0.113_{sys}$.

Contributed paper to the International Europhysics Conference on High Energy Physics (HEP-97), Jerusalem, Israel, Aug/19-26/97
Reference number: EPS-123

[1]This work was supported by Department of Energy contracts: DE-FG02-91ER40676 (BU), DE-FG03-92ER40701 (CIT), DE-FG03-91ER40618 (UCSB), DE-FG03-92ER40689 (UCSC), DE-FG03-93ER40788 (CSU), DE-FG02-91ER40672 (Colorado), DE-FG02-91ER40677 (Illinois), DE-AC03-76SF00098 (LBL), DE-FG02-92ER40715 (Massachusetts), DE-AC02-76ER03069 (MIT), DE-FG06-85ER40224 (Oregon), DE-AC03-76SF00515 (SLAC), DE-FG05-91ER40627 (Tennessee), DE-AC02-76ER00881 (Wisconsin), DE-FG02-92ER40704 (Yale); National Science Foundation grants: PHY-91-13428 (UCSC), PHY-89-21320 (Columbia), PHY-92-04239 (Cincinnati), PHY-88-17930 (Rutgers), PHY-88-19316 (Vanderbilt), PHY-92-03212 (Washington); the UK Particle Physics and Astronomy Research Council (Brunel and RAL); the Istituto Nazionale di Fisica Nucleare of Italy (Bologna, Ferrara, Frascati, Pisa, Padova, Perugia); and the Japan-US Cooperative Research Project on High Energy Physics (Nagoya, Tohoku).

1 Introduction

Parity violation in $Z^0 \to f\overline{f}$ couplings can be expressed in terms of the combination of vector (v) and axial vector (a) couplings of the fermion f to the Z^0, as $A_f = 2v_f a_f/(v_f^2 + a_f^2)$. It is especially interesting to pursue measurements of A_b as a probe of the $Zb\overline{b}$ coupling, complementary to the measurements of $R_b = \Gamma(Z^0 \to b\overline{b})/\Gamma(Z^0 \to Hadrons)$. A_b is particularly sensitive to possible deviations in the right-handed $Zb\overline{b}$ coupling predicted by the standard model. With the availability of the longitudinal electron beam polarization P_e, it is possible to measure A_b from the the left-right forward-backward asymmetry for $e^+e^- \to Z^0 \to b\overline{b}$ events,

$$\tilde{A}^b_{FB}(z) = \frac{[\sigma^b_L(z) - \sigma^b_L(-z)] - [\sigma^b_R(z) - \sigma^b_R(-z)]}{[\sigma^b_L(z) + \sigma^b_L(-z)] + [\sigma^b_R(z) + \sigma^b_R(-z)]} = |P_e| A_b \frac{2z}{1+z^2}, \tag{1}$$

where L, R refer to $Z^0 \to b\overline{b}$ decays produced with a predominantly left-handed (negative helicity) or right-handed (positive helicity) electrons, respectively and $z = \cos\theta$ for b quark production at polar angle θ from the electron beam direction. This formulation of a double asymmetry removes the dependence on the Zee coupling parameter A_e and measures A_b from the the final state $Zb\overline{b}$ coupling directly. The large value of $|P_e|$ from a highly polarized electron beam also produces a large raw asymmetry with enhanced sensitivity to A_b.

Direct measurements of A_b using left-right forward-backward asymmetries have been performed previously by SLD, in which the b quark charge was determined using momentum weighted track charge combined with a lifetime b-tag [1] or the sign of decay leptons [2]. In this paper, we present a new technique for signing the b quark direction using identified charged kaons. The basic idea of tagging the parent $B/\overline{B}$ meson production through the sign of a charged kaon in the B cascade decay chain has been promoted as a major new technique for many future experimental facilities. With the successful operation of the SLD Cerenkov Ring Imaging Detector for particle identification, we are able to apply this technique for this b asymmetry measurement.

The main sources of charged kaon production in B meson decays can be classified as:

$$\begin{array}{llll}
\overline{B} \to DX & \text{and} & D \to K^- & (a) \\
\overline{B} \to D/\psi X & \text{and} & X \text{ contains } K^- & (b) \\
\overline{B} \to D\overline{D}_{(s)}X & \text{and} & \overline{D}_{(s)} \to K^- & (c) \\
\overline{B} \to D\overline{D}X & \text{and} & X \to K^- & (d) \\
\overline{B} \to DX & \text{and} & D \to K^+ & (e) \\
\overline{B} \to D/\psi X & \text{and} & X \text{ contains } K^+ & (f) \\
\overline{B} \to D\overline{D}_s X & \text{and} & \overline{D}_s \to K^+ & (g)
\end{array}$$

where ψ represents all charmonia. The source (a) represents the main decay cascade chain of $b \to c \to s$ and is expected to be the dominant source of the kaon production. The sign of the kaon charge therefore provides the $B/\overline{B}$ separation with K^- tagging the b quark in $\overline{B}$ meson, and K^+ tagging the $\overline{b}$ anti-quark in B meson. In the remainder of this paper, whenever we discuss the $K^\pm$ production from $\overline{B}$ mesons, the charge conjugate modes are also implied. The kaon sources $(a - d)$ are therefore 'right-sign' sources and $(e - g)$ are 'wrong-sign' sources. Although the K^- tags b-quark at decay, the neutral B meson mixing dilutes the analysing power for tagging b quark at production in a similar manner as for other asymmetry measurement techniques.

2 Experimental Setup and Monte Carlo Simulation

The operation of the SLAC Linear Collider (SLC) with a polarized electron beam has been described previously [3]. During the 1994-1995 running period, SLD recorded 100,000 hadronic Z^0 decays at a mean center of mass energy of 91.26 GeV with a longitudinal electron beam polarization of 77.2±0.6%. Charged particle tracking is provided by the Central Drift Chamber (CDC) [4] and a CCD based pixel vertex detector (VXD) [5], residing within a uniform axial magnetic field of 0.6T. The track impact parameter resolution in the $r\phi$ (rz) plane is $11\mu m$ ($37\ \mu m$) at high momentum and $76\mu m$ ($80\ \mu m$) at $\frac{P}{sin^{3/2}\theta}$=1 GeV/c. The small and stable SLC interaction point in $r\phi$ is tracked continuously averaging over ~30 hadronic Z^0 events, with a resulting effective event primary vertex resolution of $7\mu m$. The event primary vertex z location is determined event by event with an average precision of $35\mu m$. A more detailed description of the tracking system performance and primary vertex determination can be found in [6]. The Liquid Argon Calorimeter (LAC) [7] is used for the triggering and selection of the events, as well as for determination of the event thrust axis.

Central to this analysis is the SLD Cerenkov Ring Imaging Detector (CRID) [8] for particle identification. The barrel CRID uses liquid C_6F_{14} and gaseous C_5F_{12} as radiators. The Cerenkov photons from both radiators are imaged into time projection chambers (TPC) containing photosensitive gas. This analysis uses data from both barrel CRID gas and liquid radiators for $\pi/K/p$ separation in the 1-20 GeV momentum region, over the polar angle range of $cos\theta \leq 0.68$. The average detected Cerenkov photon yield for highly relativistic charged particles are 9.2 (12.8) per full ring for gas (liquid) rings. The measured refractive index for the gas (liquid) radiator is 1.00172 (1.282), corresponding to $\pi/K/p$ thresholds of 2.4/8.4/16.0 (0.17/0.62/1.17) GeV/c. The measured gas (liquid) ring angular resolution is 3.8 (13) mrad, consistent with the design value. The barrel CRID was operational with normal high voltage for 92% of the 94-95 data and on average 95% of the detector channels were fully functional. A detailed description of the particle identification performance can be found in section 4.

The $Z^0 \rightarrow Hadrons$ Monte Carlo (MC) events are simulated using the JETSET 7.4 [9] generator framework. The decays of D^0, D^+, D_s mesons and Λ_c baryons are simulated with according to measured exclusively branching ratios as listed in the particle data group review [10]. Some unmeasured decay modes are also included with branching ratios according to expectations from isospin symmetry and decay modes with large measurement errors are adjusted within tolerance to reproduce the observed inclusive particle production rates. The decays of weakly decaying charm baryons other than Λ_c are simulated using the JETSET 7.4 heavy flavor decay package. The b baryon decay simulation also uses the unmodified JETSET 7.4 heavy hadron decay package, while the B meson decay simulation is based on the QQ Monte Carlo program from CLEO [11]. Within this model, the semileptonic B decays are simulated using the ISGW [12] form factor model with a 23% D^{**} production fraction, which provides a good description of the CLEO data [13]. The hadronic B decay model was tuned to reproduce the CLEO inclusive measurements of charm meson production

[14], charm baryon production [15] and charmonium production [16]. We have adjusted the W fragmentation $s\bar{s}$ popping fraction and vector/pseudoscalar production ratio in the B decay model, so that the momentum spectra of $\pi^{\pm}$, $K^{\pm}$, K^0 and protons in the B decay rest frame and their production rates for average B_u, B_d decays in the MC are in good agreement with the ARGUS measurements [17].

The MC production fractions of different species of B hadrons are $B_u : B_d : B_s : b - baryon = 40.6 : 40.6 : 11.5 : 7.3$. All mean decay lifetimes of charm hadrons used in the MC are from the 1994 Particle Data Group review [10]. The mean decay lifetime of B hadrons in the MC are set to $1.55ps$ for B mesons and $1.10ps$ for b baryons. The neutral B meson mixing simulation used $\Delta m_d/\Gamma_d = 0.75$ and $\Delta m_s/\Gamma_s = 10$.

The MC detector simulation is based on GEANT 3.21, with a detailed geometric and material description of the SLD, and produces data that models the detector response to charged and neutral particles. Simulated Z^0 events are overlaid with noise from events taken on random beam crossings in close time-proximity to each recorded real Z^0 and then processed using the same reconstruction algorithm as for the data.

3 Event and Track Selection

The hadronic Z^0 decay events are selected with the following requirements:

- Total Visible energy in events from charged tracks > 18 GeV.
- Event thrust axis reconstructed from calorimeter clusters satisfy $|cos\theta_{thrust}| < 0.70$.
- Number of CDC tracks ≥ 7.
- CDC,VXD and CRID all in normal operation.

A fiducial set of 54638 Z^0 events is obtained from the 1994-95 data. The corresponding sample of MC events is 177K, plus an additional 168K $b\bar{b}$ only MC events.

A set of 'quality tracks' is selected for both the purpose of tagging the $b\bar{b}$ events and kaon identification. The quality track requirements are:

- Momentum transverse to beam line $P_t > 0.4$ GeV/c.
- $|cos\theta| < 0.8$.
- Innermost CDC hit at radius $R <$39cm and number of CDC hits $\geq$40.
- CDC track fit $\chi^2/NDF < 5$.
- Track must have at least one VXD hit.
- Combined CDC+VXD track fit $\chi^2/NDF < 5$.

- Estimated track $r\phi$ impact parameter resolution $< 250\mu m$.
- Impact parameter to primary vertex <3mm in both $r\phi$ and rz views.

There are $\sim$4% more tracks in the MC passing the quality track selection than in the data. This is assumed to be an extra tracking inefficiency not simulated in the MC, so that a correction procedure is used to randomly remove tracks from the MC as a function of track momentum, ϕ and cosθ to match the data.

4 $K^{\pm}$ Identification

To ensure the availability of CRID data for particle identification, the track selection for kaon identification include the following requirements in addition to the standard quality track selection:

- Momentum of track in the range 1 GeV $< P <$ 20 GeV.
- Track $|cos\theta| < 0.67$ (0.64) for particle ID with gas (liquid) radiator data.
- For the gas radiator data (3-20 GeV), the track is required to have an associated minimum ionizing particle (MIP) signal in the CRID TPC or have a liquid ring with at least 4 hits. Further more, the TPC region where gas ring hits are expected required not to contain too many hits from saturated MIP signals.
- For the liquid radiator data (1-6 GeV), the track is required to have an associated MIP signal in the CRID TPC if the track is traversing through an active TPC volume.

The fraction of quality tracks in the fiducial volume passing the last two selection criteria is 75% (81%) for gas (liquid) data, in good agreement with the fraction of 77% (81%) in the MC.

Charged particle identification with the CRID is performed using a likelihood technique [18]. For each of the charged particle hypotheses a likelihood is calculated based upon the number of detected photo-electrons and their measured Cerenkov angles compared to the expectations for this hypothesis. This likelihood calculation takes into account the effects of locally measured background including that due to overlapping rings. Particle separation is based upon differences between logarithms of the likelihoods, L_π, L_K and L_P for pion, kaon and proton hypotheses respectively, combining the gas and liquid information. The $K^{\pm}$ candidate tracks are selected requiring $L_K - L_\pi >$ 5,4,3 respectively for tracks in the momentum ranges of 1.0-2.5, 2.5-3.0,3.0-20.0 GeV. Proton rejection is made by requiring $L_K - L_P > -3$. The $L_K - L_\pi$ distributions for electrons and muons are very similar to pions for most of the momentum ranges and are included in the "pion" class for all the following discussions on particle identification. The $L_K - L_\pi$ distribution for tracks in the momentum region 3-7 GeV is shown in Fig.1 as an example. This is in fact the momentum region containing most of the B decay kaons. The main particle ID discrimination in this region comes from the gas radiator threshold effect, i.e., pions have rings while the momentum is not high enough for kaons and protons to produce Cerenkov light for gas rings.

The asymmetry measurement presented in this paper is relatively insensitive to the efficiency for identifying real kaons, while it is more sensitive to the fraction of other particles (mainly pions) in the kaon candidate sample due to misidentification. It can be seen in Fig.1 that the MC simulation of the particle likelihood does not perfectly represent data, so that a calibration of the $\pi \to K$ misidentification rate is performed using $\pi^{\pm}$ tracks from identified high purity $K_s \to \pi^+\pi^-$ decays in hadronic Z^0 events, as well as the 3-prong τ decays in $Z^0 \to \tau\tau$ data events. Charged particles from 3-prong τ decays are mainly pions, while the decay modes producing kaons sum to a rather small and quite well measured total branching ratio. The track density in 3-prong τ decays is also similar to the jet environment in hadronic Z^0 events. The $\pi \to K$ mis-ID rates range from $\sim$1.5% at low momentum to 8-12% at high momentum. The kaon selection cuts on $L_K - L_\pi$ for true π, e, μ in the MC are adjusted until the $\pi \to K$ mis-ID rate matches that of the data with nominal cuts. These adjustments are sufficiently small that the effect due to the changes in the kaon identification efficiency is negligible. We have also checked that the $cos\theta$ dependence of the mis-ID effects as seen in the calibration data samples agrees with the MC.

5 b-tag and B decay track selection

To isolate the kaons from B decays for the asymmetry measurement, b events are tagged using a B vertex mass reconstruction technique [19], which also provides a clean selection of B decay tracks.

Events are divided into two hemispheres by the plane perpendicular to the thrust axis (calculated from calorimeter energy clusters). A topological vertex reconstruction procedure [20] for finding seconardy vertices is applied separately to the quality tracks in each hemisphere. A seed vertex (SV) is chosen as the secondary vertex with the highest vertex significance reflecting track overlap density. The SV is required to have a distance to the PV >1mm and contain at least 2 tracks with 3D impact parameter to the PV $>130\mu m$. Vertices consistent with originating from $K_s \to \pi^+\pi^-$ decays are rejected.

Since not all B decay tracks necessarily originate from the same vertex, other quality tracks are then tested for compatibility of originating from B decay. The line between the PV and SV is defined as the vertex axis with a PV to SV distance D. At the 3D point of closest approach to the vertex axis for each quality track, the transverse distance between the axis and the track is denoted as T and the longitudinal distance from PV to this point is denoted as L. Tracks with $T <$1mm, $L >$1mm and $L/D > 0.25$ are included as B decay tracks for the B mass calculation. The above procedure is illustrated in Fig.2.

All selected B decay tracks are assigned a pion mass to calculate a raw B mass M_{raw}. Kinematic information is then added based on the missing P_T calculated from the angle between the vertex axis (B flight direction) and the B decay track momentum sum direction. A minimal missing P_T consistent with the PV and SV errors is added to construct a corrected B mass $\mathcal{M}$ which greatly enhances the separation between b and $udsc$ events. This step benefits from the excellent resolution of both the PV and SV at SLD. A further constraint is placed on the missing P_T correction to restrict $\mathcal{M} < 2M_{raw}$ to prevent fake *uds* vertices obtaining excessive missing P_T corrections. The event is tagged as a b event when either hemisphere has $\mathcal{M} > 1.8$ GeV. There are 7597 data events satisfying the b-tag requirement corresponding to a b-tag efficiency of 57.7% and a b-purity of 95.5%, with the remaining background mainly being $c\bar{c}$ events.

Further B decay track selection cuts are made to improve the B decay track purity by requiring $T < 0.3$mm and $0.5 < L/D < 5.0$. The effectiveness of the L/D cut for B decay track selection is illustrated in Fig.3 for tracks which have passed particle ID quality cuts in b-tagged. The fraction of true B decay tracks among these selected tracks is 96%, and the primary vertex track fraction is only 1%, while the remaining tracks are from charm decays in $c\bar{c}$ background or from interactions in the detector material.

6 The Asymmetry Measurement

The charged kaon identification procedure is applied to the selected B decay tracks in the tagged hemispheres. The number of identified B decay kaon candidate tracks per tagged event, and the kaon candidate track momentum distributions are shown in Fig.4a and Fig.4b. The candidate track true kaon fraction is shown in Fig.4c as a function of track momentum. The fraction of right sign kaons for candidate tracks in true b events is shown in Fig.4d as a function of track momentum.

The charges of kaon candidates in each hemisphere are then added and a non-zero charge provides the b quark direction signing. In case the hemisphere kaon charge sum is negative (positive), the hemisphere is signed as the b quark ($\bar{b}$ anti-quark) with the thrust axis toward that hemisphere as the b ($\bar{b}$) direction. Events are not used for asymmetry analysis in case both hemispheres have the same kaon charge. There are 2963 b-tagged events in the data which have successful kaon charge signed b direction. The corresponding events in the MC indicate a correct quark direction signing fraction of 72.5% for b events in the tagged sample.

The event thrust axis $\cos\theta$ distributions as signed by the tagged kaons for b-quarks are shown in Fig.5 for events with left- and right-handed electron beam polarizations separately. The small *udsc* backgrounds as estimated from the MC are then subtracted from both the data and MC samples to obtain the polar angle distribution for pure b events. The left-right forward-backward asymmetry is then formed as a function of $cos\theta$:

$$\tilde{A}^b_{FB}(z) = \frac{N_L(z) - N_R(z) - N_L(-z) + N_R(-z)}{N_L(z) + N_R(z) + N_L(-z) + N_R(-z)}$$

where $z = |cos\theta|$ and N_L, N_R are the event populations for Left- and Right-handed beam events in the corresponding $cos\theta$ bins. The left-right forward-backward asymmetry of MC b events with the same mix of left and right-handed events according to the measured beam polarization in the data is used as the fitting function. Since the magnitude of the asymmetry in each $cos\theta$ bin is directly proportional to A_b, a common asymmetry scaling factor for all $cos\theta$ bins in the MC is allowed to vary to achieve the best χ^2 fit to the data. The fitted scaling factor is the ratio between A_b in the data and the generated A_b value in the MC.

The left-right forward-backward asymmetry distributions for the data and best fit MC are shown in Fig.6.

It should be noted that the above fitting procedure using the MC as fitting function has effectively included QCD radiative corrections as generated in the JETSET MC, and has naturally taken into account any analysis bias to the QCD correction. To be consistent with other direct measurements of A_b from SLD, we choose to quote our result using the Stav and Olsen [21] 1st order QCD correction calculation taking into account quark mass effects in the matrix elements. The change in the effective QCD correction from the JETSET calculation to Stav and Olsen calculation resulted in a correction to A_b of +0.3%. The fit result including this correction is $A_b = 0.891 \pm 0.083$ $(stat.)$.

7 Systematics

The detector and physics systematic errors are summarized in Table 1. It should be noted that due to the formulation of the double asymmetry in $\tilde{A}_{FB}$, many detector non uniformity effects cancel. The most significant detector systematic is due to the uncertainty in $\pi \rightarrow K$ mis-identification, where the calibration statistical error from $K_s^0 \rightarrow \pi^+\pi^-$ and $\tau \rightarrow$3 prong data samples are quoted as systematic error. The full effect of applying the tracking efficiency correction to the MC is also included as a systematic error.

The dominant systematic uncertainty of this measurement is due to the uncertainty in the K^+/K^- production ratio in B meson decays. We have adjusted the MC to the ARGUS measurement [17] of average B_u, B_d meson kaon production rates (including B_d mixing)

$$\overline{B} \rightarrow K^- = 0.620 \pm 0.013 \pm 0.038 \quad (2)$$
$$\overline{B} \rightarrow K^+ = 0.165 \pm 0.011 \pm 0.036 \quad (3)$$

and varied the two rates independently according to the respective experimental errors and added the errors on A_b in quadrature. This is in fact a conservative estimate as the dominant systematic errors in the ARGUS measurement contain large common sources between K^+ and K^- such as K-identification efficiency which should cancel when only considering the K^+/K^- production *ratio* as relevant for this measurement. The re-evaluation of the ARGUS results in terms of a production ratio is currently in progress within the ARGUS collaboration.

The MC B_u, B_d $K^\pm$ momentum spectra in B rest frame are reweighted to match the ARGUS data for both the spectra shape and K^+/K^- production ratio. The difference in spectrum shape between the MC and the ARGUS measurement is taken as a systematic error. For the tagged B decay kaon momentum spectrum in SLD (Fig.4b), the difference between data and MC is attributed to a kaon identification efficiency uncertainty, which is in turn translated to an error in A_b included in the kaon momentum spectrum error.

Due to the rather different nature of the B_s and b baryon decays, their production rate uncertainties have noticeable effects on the estimated overall kaon candidate b-quark signing analysing power. In the case of B_s decays, not only the K^+ and K^- tend to be symmetric for either final state flavor, the rapid B_s oscillation further randomizes the kaon sign correlation with initial quark flavor so that the K^+ and K^- production is almost completely symmetric. The main source of uncertainty is therefore just the B_s production rate. The proton production from b-baryons is a potential source of systematic, due to the limited K/P separation in the CRID gas threshold region and the proton from b-baryon decays tend to be the wrong charge compared to right sign kaons from B mesons. However, the fact that a large fraction of the protons originate from subsequent Λ decays results in a reduced sensitivity since Λ decay tracks tend to fail the quality track selection or the B track selection procedure.

The uncertainty in the charm background fraction is estimated in a similar manner as in Ref.[19]. The very small effect on R_b from the the charm background fraction uncertainty is due to the rather small charm background fraction and the interesting fact that kaons from $c \to s$ have the same sign as those from $b \to c \to s$ such that the magnitude of the raw kaon asymmetries for $b\bar{b}$ and $c\bar{c}$ events are very similar. It should be noted that this is in contrast with the jet-charge and lepton final state tags where the charm backgrounds have the wrong sign compared to the main signal source from b. The charm meson decay kaon yield uncertainties estimated based on the MK-III measurement [22] also has rather small effects.

The systematic error due to the QCD correction, includes uncertainties in the 2nd order QCD corrections and α_s, uncertainties in the bias due to selection criteria in the analysis, as well as explicitly evaluated effects of gluon splitting to heavy quark pairs.

8 Conclusions

In summary, we have performed a direct measurement of A_b from the left-right forward-backward asymmetry using the highly polarized electron beam at SLC. This measurement demonstrates the effectiveness of a new technique of final state b flavor tagging using kaons identified by the SLD CRID together with a high purity b-tag using the CCD pixel vertex detector. From 100K hadronic Z^0 events collected by SLD during 1994-1995, we obtain a preliminary result of

$$A_b = 0.891 \pm 0.083_{stat} \pm 0.113_{sys}$$

This result is consistent with the Standard Model expectation of 0.935 and in good agreement with other direct measurements of A_b [23]. The systematic uncertainties are very different compared to other measurement techniques and is expected to decrease significantly once a re-evaluation of the existing ARGUS measurement of kaon production in B decays is completed.

9 Acknowledgments

We thank the personnel of the SLAC accelerator department and the technical staffs of our collaborating institutions for their outstanding efforts on our behalf.

The SLD Collaboration

* List of Authors

K. Abe,[19] K. Abe,[29] I. Adam,[27] T. Akagi,[27] N. Allen,[4] W.W. Ash,[27] D. Aston,[27] K.G. Baird,[16] C. Baltay,[33] H.R. Band,[32] M.B. Barakat,[33] O. Bardon,[16] T. Barklow,[27] A.O. Bazarko,[11] R. Ben-David,[33] A.C. Benvenuti,[2] G.M. Bilei,[22] D. Bisello,[21] G. Blaylock,[7] J.R. Bogart,[27] B. Bolen,[17] T. Bolton,[11] G.R. Bower,[27] J.E. Brau,[20] M. Breidenbach,[27] W.M. Bugg,[28] D. Burke,[27] T.H. Burnett,[31] P.N. Burrows,[16] W. Busza,[16] A. Calcaterra,[13] D.O. Caldwell,[6] D. Calloway,[27] B. Camanzi,[12] M. Carpinelli,[23] R. Cassell,[27] R. Castaldi,[23] A. Castro,[21] M. Cavalli-Sforza,[7] A. Chou,[27] E. Church,[31] H.O. Cohn,[28] J.A. Coller,[3] V. Cook,[31] R. Cotton,[4] R.F. Cowan,[16] D.G. Coyne,[7] G. Crawford,[27] A. D'Oliveira,[8] C.J.S. Damerell,[25] S. Dasu,[27] M. Daoudi,[27] N. De Groot,[27] R. De Sangro,[13] R. Dell'Orso,[23] M. Dima,[9] P. Dervan,[4] D.N. Dong,[16] P.Y.C. Du,[28] R. Dubois,[27] B.I. Eisenstein,[14] V. Onno Eschenburg,[18] E. Etzion,[32] S. Fahey,[10] D. Falciai,[22] C. Fan,[10] M.J. Fero,[16] K. Flood,[17] R. Frey,[20] T. Gillman,[25] G. Gladding,[14] S. Gonzalez,[16] E.L. Hart,[28] J.L. Harton,[9] A. Hasan,[4] Y. Hasegawa,[29] K. Hasuko,[29] S. Hedges,[4] S.S. Hertzbach,[17] M.D. Hildreth,[27] J. Huber,[20] M.E. Huffer,[27] E.W. Hughes,[27] X. Huynh,[27] H. Hwang,[20] Y. Iwasaki,[29] D. Jackson,[25] P. Jacques,[24] J. Jaros,[27] A.S. Johnson,[3] J.R. Johnson,[32] R.A. Johnson,[8] T. Junk,[27] R. Kajikawa,[19] M. Kalelkar,[24] Y. Kamyshkov,[28] H.J. Kang,[34] I. Karliner,[14] H. Kawahara,[27] H.W. Kendall,[16] Y. Kim,[26] M.E. King,[27] R. King,[27] R.R. Kofler,[17] N.M. Krishna,[10] R.S. Kroeger,[18] J.F. Labs,[27] M. Langston,[20] A. Lath,[16] J.A. Lauber,[10] D.W.G. Leith,[27] V. Lia,[16] X. Liu,[7] M. Loreti,[21] A. Lu,[6] H.L. Lynch,[27] J. Ma,[31] G. Mancinelli,[24] S. Manly,[33] G. Mantovani,[22] T.W. Markiewicz,[27] T. Maruyama,[27] H. Masuda,[27] E. Mazzucato,[12] A.K. McKemey,[4] B.T. Meadows,[8] G. Menegatti,[12] R. Messner,[27] P.M. Mockett,[31] K.C. Moffeit,[27] T. Moore,[33] D. Muller,[27] T. Nagamine,[27] S. Narita,[29] U. Nauenberg,[10] H. Neal,[27] M. Nussbaum,[8] Y. Ohnishi,[19] N. Oishi,[19] D. Onoprienko,[28] L.S. Osborne,[16] R.S. Panvini,[30] H. Park,[20] C.H. Park,[35] T.J. Pavel,[27] I. Peruzzi,[13] M. Piccolo,[13] L. Piemontese,[12] E. Pieroni,[23] K.T. Pitts,[20] R.J. Plano,[24] R. Prepost,[32] C.Y. Prescott,[27] G.D. Punkar,[27] J. Quigley,[16] B.N. Ratcliff,[27] T.W. Reeves,[30] J. Reidy,[18] P.L. Reinertsen,[7] P.E. Rensing,[27] L.S. Rochester,[27] P.C. Rowson,[11] J.J. Russell,[27] O.H. Saxton,[27] T. Schalk,[7] R.H. Schindler,[27] U. Schneekloth,[16] B.A. Schumm,[15] J. Schwiening,[27] S. Sen,[33] V.V. Serbo,[32] M.H. Shaevitz,[11] J.T. Shank,[3] G. Shapiro,[15] D.J. Sherden,[27] K.D. Shmakov,[28] C. Simopoulos,[27] N.B. Sinev,[20] S.R. Smith,[27] M.B. Smy,[9] J.A. Snyder,[33] H. Staengle,[9] P. Stamer,[24] H. Steiner,[15] R. Steiner,[1] M.G. Strauss,[17] D. Su,[27] F. Suekane,[29] A. Sugiyama,[19] S. Suzuki,[19] M. Swartz,[27] A. Szumilo,[31] T. Takahashi,[27] F.E. Taylor,[16] E. Torrence,[16] A.I. Trandafir,[17] J.D. Turk,[33] T. Usher,[27] C. Vannini,[xx] J. Va'vra,[27] C. Vannini,[23] E. Vella,[27] J.P. Venuti,[30] R. Verdier,[16] P.G. Verdini,[23] S.R. Wagner,[27] D.L. Wagner,[10] A.P. Waite,[27] J. Wang,[27] C. Ward,[4] S.J. Watts,[4] A.W. Weidemann,[28] E.R. Weiss,[31] J.S. Whitaker,[3] S.L. White,[28] F.J. Wickens,[25] D.C. Williams,[16] S.H. Williams,[27] S. Willocq,[27] R.J. Wilson,[9] W.J. Wisniewski,[5] M. Woods,[27] G.B. Word,[24] T.R. Wright,[32] J. Wyss,[21] R.K. Yamamoto,[16] J.M. Yamartino,[16] X. Yang,[20] J. Yashima,[29] S.J. Yellin,[6] C.C. Young,[27] H. Yuta,[29] G. Zapalac,[32] R.W. Zdarko,[27] and J. Zhou[20]

[1] Adelphi University, Garden City, New York 11530
[2] INFN Sezione di Bologna, I-40126 Bologna, Italy
[3] Boston University, Boston, Massachusetts 02215
[4] Brunel University, Uxbridge, Middlesex UB8 3PH, United Kingdom
[5] California Institute of Technology, Pasadena, California 91125
[6] University of California at Santa Barbara, Santa Barbara, California 93106
[7] University of California at Santa Cruz, Santa Cruz, California 95064
[8] University of Cincinnati, Cincinnati, Ohio 45221
[9] Colorado State University, Fort Collins, Colorado 80523
[10] University of Colorado, Boulder, Colorado 80309
[11] Columbia University, New York, New York 10027
[12] INFN Sezione di Ferrara and Università di Ferrara, I-44100 Ferrara, Italy
[13] INFN Lab. Nazionali di Frascati, I-00044 Frascati, Italy
[14] University of Illinois, Urbana, Illinois 61801
[15] Lawrence Berkeley Laboratory, University of California, Berkeley, California 94720
[16] Massachusetts Institute of Technology, Cambridge, Massachusetts 02139
[17] University of Massachusetts, Amherst, Massachusetts 01003
[18] University of Mississippi, University, Mississippi 38677
[19] Nagoya University, Chikusa-ku, Nagoya 464 Japan
[20] University of Oregon, Eugene, Oregon 97403
[21] INFN Sezione di Padova and Università di Padova, I-35100 Padova, Italy
[22] INFN Sezione di Perugia and Università di Perugia, I-06100 Perugia, Italy
[23] INFN Sezione di Pisa and Università di Pisa, I-56100 Pisa, Italy
[24] Rutgers University, Piscataway, New Jersey 08855
[25] Rutherford Appleton Laboratory, Chilton, Didcot, Oxon OX11 0QX United Kingdom
[26] Sogang University, Seoul, Korea
[27] Stanford Linear Accelerator Center, Stanford University, Stanford, California 94309
[28] University of Tennessee, Knoxville, Tennessee 37996
[29] Tohoku University, Sendai 980 Japan
[30] Vanderbilt University, Nashville, Tennessee 37235
[31] University of Washington, Seattle, Washington 98195
[32] University of Wisconsin, Madison, Wisconsin 53706
[33] Yale University, New Haven, Connecticut 06511
[33] Yale University, New Haven, Connecticut 06511
[34] Sogang University, Seoul, Korea
[35] Soongsil University, Seoul, Korea

References

[1] SLD Collab.: K. Abe *et al.* *Phys. Rev. Lett.* **74** (1995) 2890

[2] SLD Collab.: K. Abe *et al.* *Phys. Rev. Lett.* **74** (1995) 2895

[3] SLD Collab.: K. Abe *et al.* *Phys. Rev. Lett.* **73** (1994) 25;
SLD Collab.: K. Abe *et al.* *Phys. Rev. Lett.* **78** (1997) 2075.

[4] M. D. Hildreth *et al.*, *Nucl. Instr. & Meth.* **A367**, 111 (1995); & *IEEE Trans. Nucl. Sci.* **42**, 451 (1995).

[5] G. Agnew *et al.*, SLAC-PUB-5906, *Proceedings of the 26th Internaltional Conference on High Energy Physics, Dallas, Texas, USA, Aug-1992*

[6] SLD Collab.: K. Abe *et al.* *Phys. Rev.* **D53** (1996) 1023.

[7] D. Axen *et al.*, *Nucl. Instr. & Meth.* **A238**, 472 (1993).

[8] K. Abe *et al.*, *Nucl. Instr. & Meth.* **A343**, 74 (1994).

[9] T. Sjöstrand *et al.*, *Comp. Phys. Comm.* **82**, 74 (1994).

[10] The Particle Data Group, *Phys. Rev.* **D50**, Part I (1994).

[11] CLEO QQ MC code provided by P. Kim and CLEO Collaboration.

[12] N. Isgur, D. Scora, B. Grinstein, and M. B. Wise, *Phys. Rev.* **D39**, 799 (1989)

[13] CLEO Collab.: B. Barish *et al.*, *Phys. Rev. Lett.* **76** (1996) 1570.

[14] CLEO Collab.: L. Gibbons *et al.*, CLNS-96-1454, *submitted to Phys. Rev. D.*

[15] CLEO Collab.: G. Crawford *et al.*, *Phys. Rev.* **D45**, 752 (1992).

[16] CLEO Collab.: D. Bortoletto *et al.*, *Phys. Rev.* **D45**, 21 (1992).

[17] ARGUS Collab.: H. Albrecht *et al.*, *Z. Phys.* **C58**, 191 (1993);
ARGUS Collab.: H. Albrecht *et al.*, *Z. Phys.* **C62**, 371 (1994).

[18] K. Abe *et al.*, *Nucl. Instr. & Meth.* **A371**, 195 (1996).

[19] SLD Collab.: K. Abe *et al.* SLAC-PUB-7481 *Submitted to Phys. Rev. Lett.*.

[20] D. J. Jackson, *Nucl. Instr. & Meth.* **A388**, 247 (1997).

[21] J. B. Stav and H. .A. Olsen, *Phys. Rev.* **D52**, 1359 (1995); *Phys. Rev.* **D50**, 6775 (1994).

[22] MK-III Collab.: D. Coffman *et al.*, *Phys. Lett.* **B263**, 135 (1991).

[23] SLD Collab.: K. Abe *et al.* SLAC-PUB-7629, EPS-122, *submitted to the International Europhysics Conference on High Energy Physics (HEP-97)*;
SLD Collab.: K. Abe *et al.* SLAC-PUB-7635, EPS-124, *submitted to the International Europhysics Conference on High Energy Physics (HEP-97)*

Systematic source		$\frac{\delta A_b}{A_b}$ (%)
K^- multiplicity from B_u/B_d	0.620±0.040	-5.0
K^+ multiplicity from B_u/B_d	0.165±0.038	10.9
Proton multiplicity in B meson decay	0.055±0.005	0.3
Kaon momentum spectrum		1.8
b fragmentation	$< X_E >$=0.697±0.008	-0.3
$b \to B_s$ production	11.5±1.8%	1.6
$b \to b$ baryon production	10.0±4.0%	2.4
Fraction $B_s \to D_s$ + X	67±20%	0.1
Fraction b baryon $\to$ c baryon + X	77±15%	0.1
b event tag charm purity	±15%	-0.1
A_c	0.67±0.07	0.7
$c\bar{c}$ charm hadron decay K^-, K^+ yield		0.3
Fragmentation $K^\pm$ production	±15%	-0.3
Physics systematic sub total		12.4
$\pi \to K$ mis-ID calibration		0.8
MC Tracking efficiency		0.3
MC statistics		1.5
Beam polarization	77.2±0.6%	-0.8
QCD corrections		0.5
Total systematic uncertainty		12.7

Table 1: List of systematic errors on measured A_b.

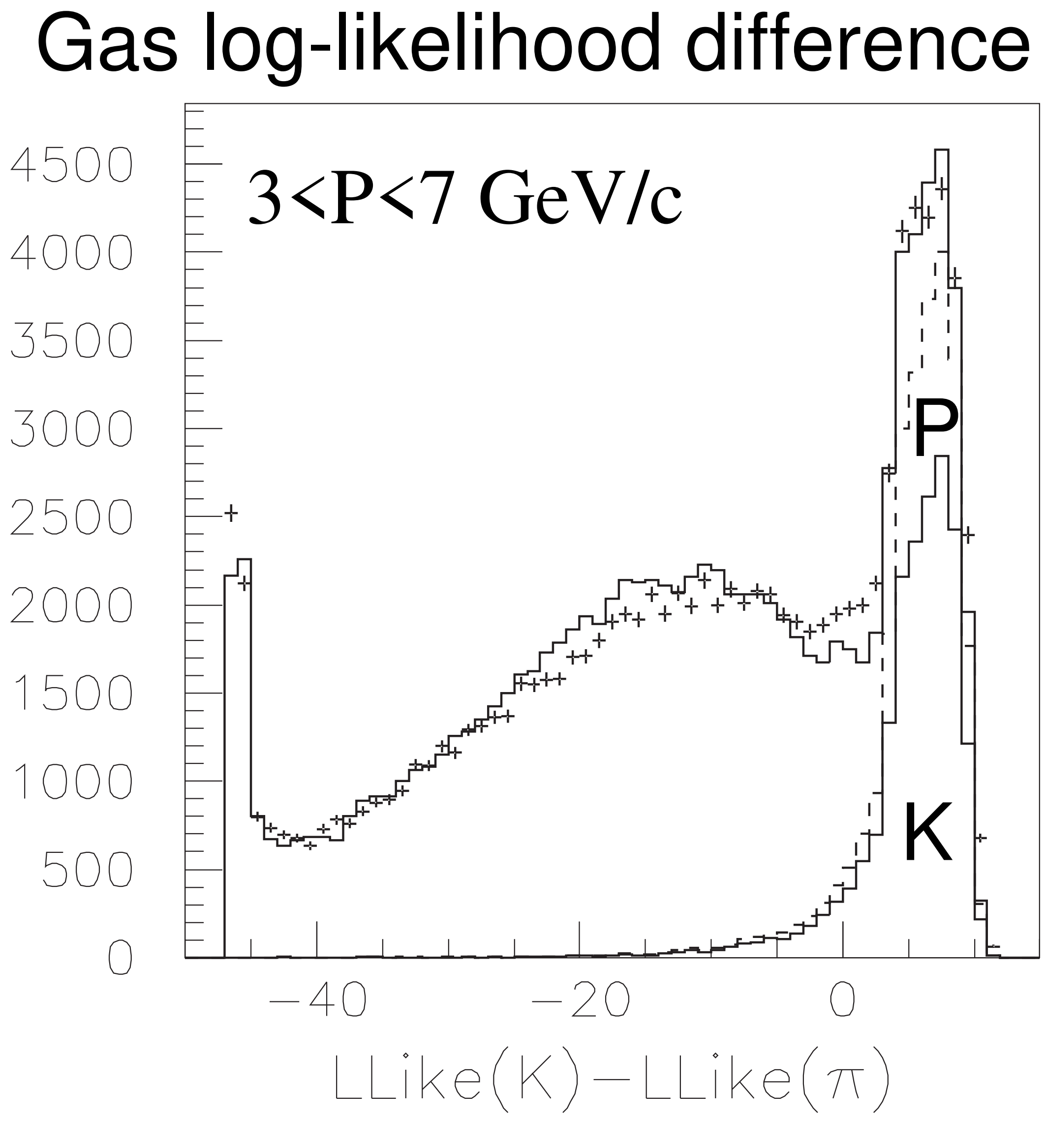

Figure 1: Distribution of log-likelihood differences between K and π hypotheses in the CRID gas radiator data for tracks in all hadronic events compared between data (crosses) and MC (histograms) together with separate distributions of various true particle types in the MC.

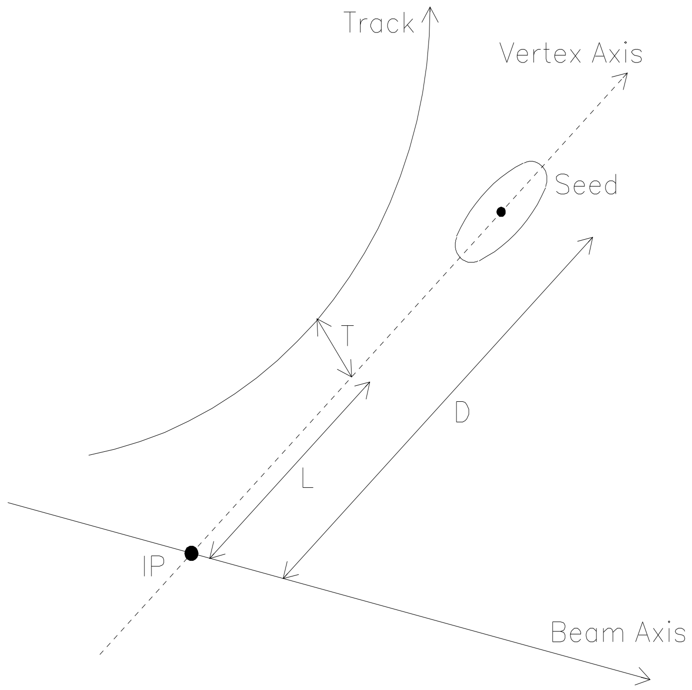

Figure 2: An illustration of the B decay track classification procedure indicating variables used for track attachment to the seed secondary vertex.

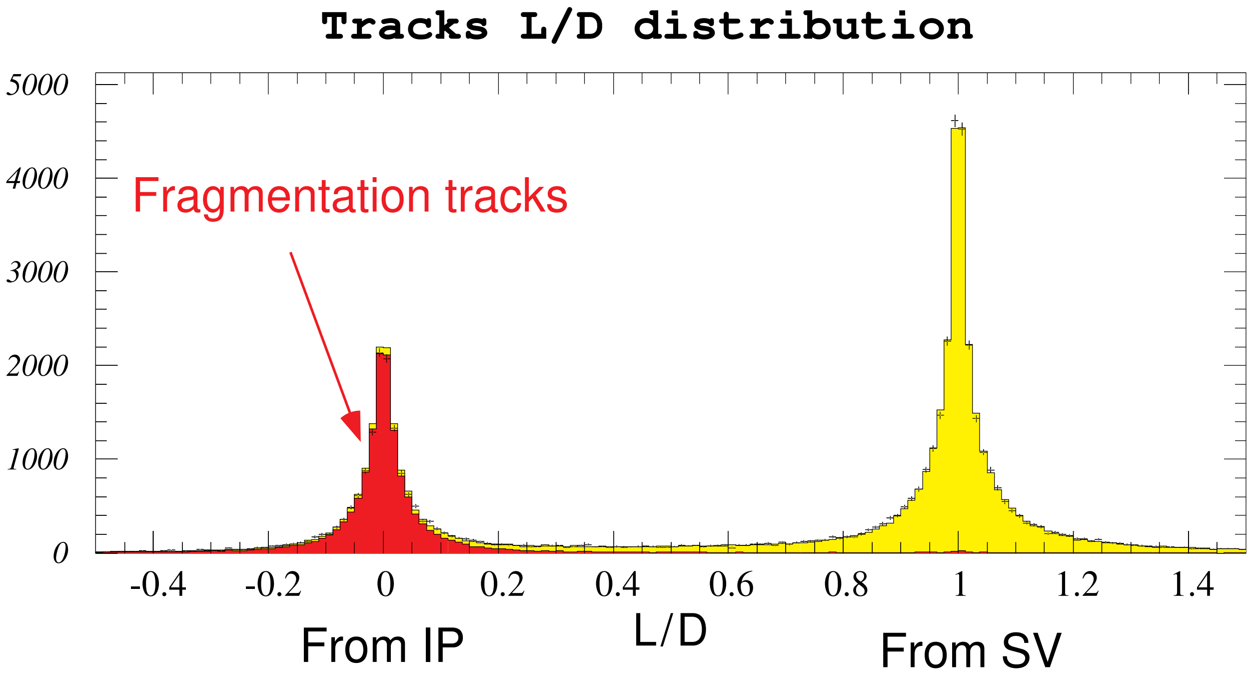

Figure 3: Distribution of track longitudinal position L/D w.r.t. seed vertex in hemispheres containing a secondary vertex. Crosses are data points and histograms are from MC, with dark shaded and light shaded region representing MC primary and secondary tracks respectively.

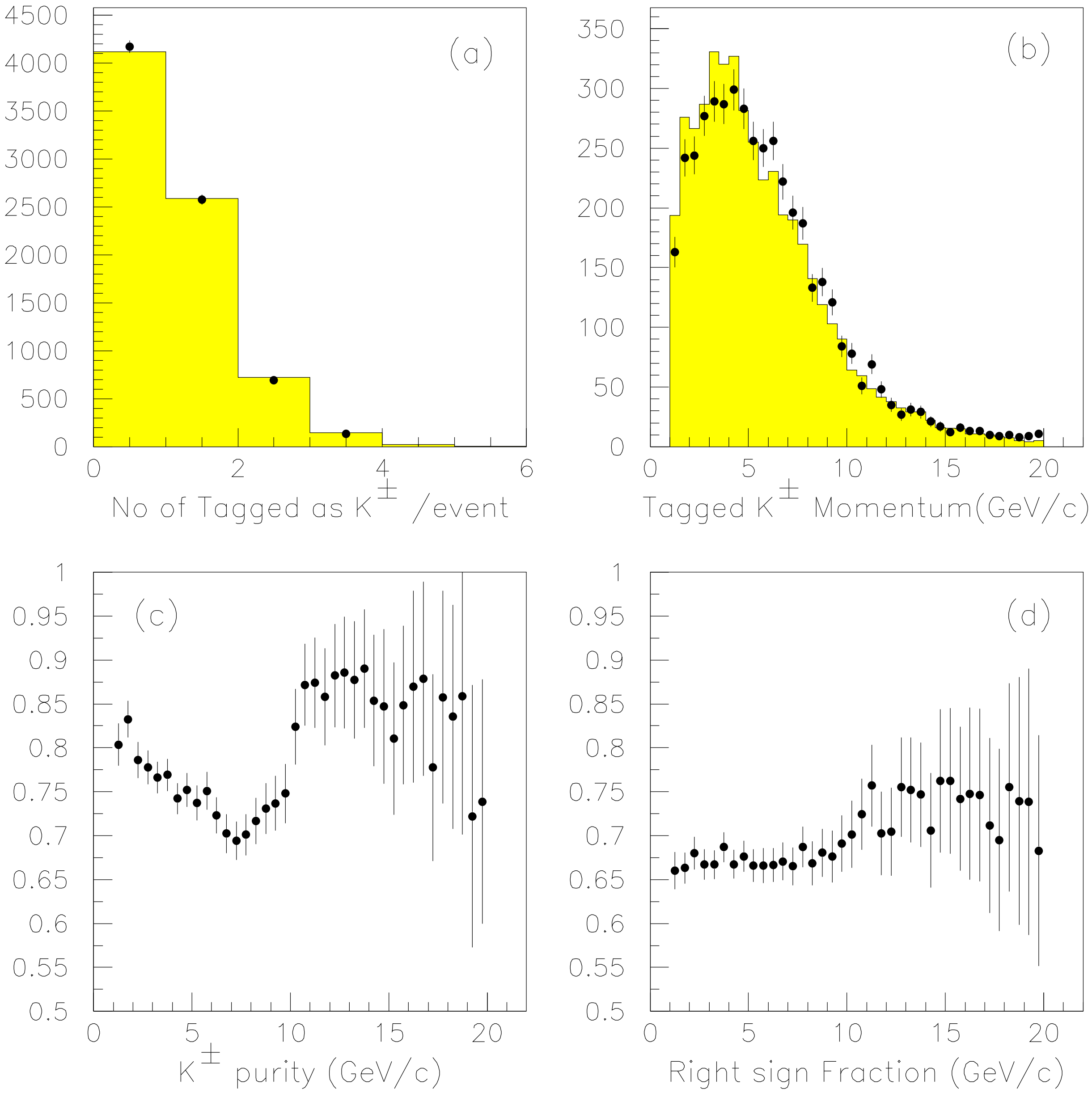

Figure 4: Distributions of a) multiplicity of identified B decay kaon candidates in b-tagged events, where points are data and histogram is MC; b) momentum distribution of identified B decay kaon candidates, where points are data and histogram is MC; c) MC true kaon fraction in identified B decay kaon candidates as a function of track momentum; d) fraction of right sign tracks in identified B decay kaon candidates as a function of track momentum.

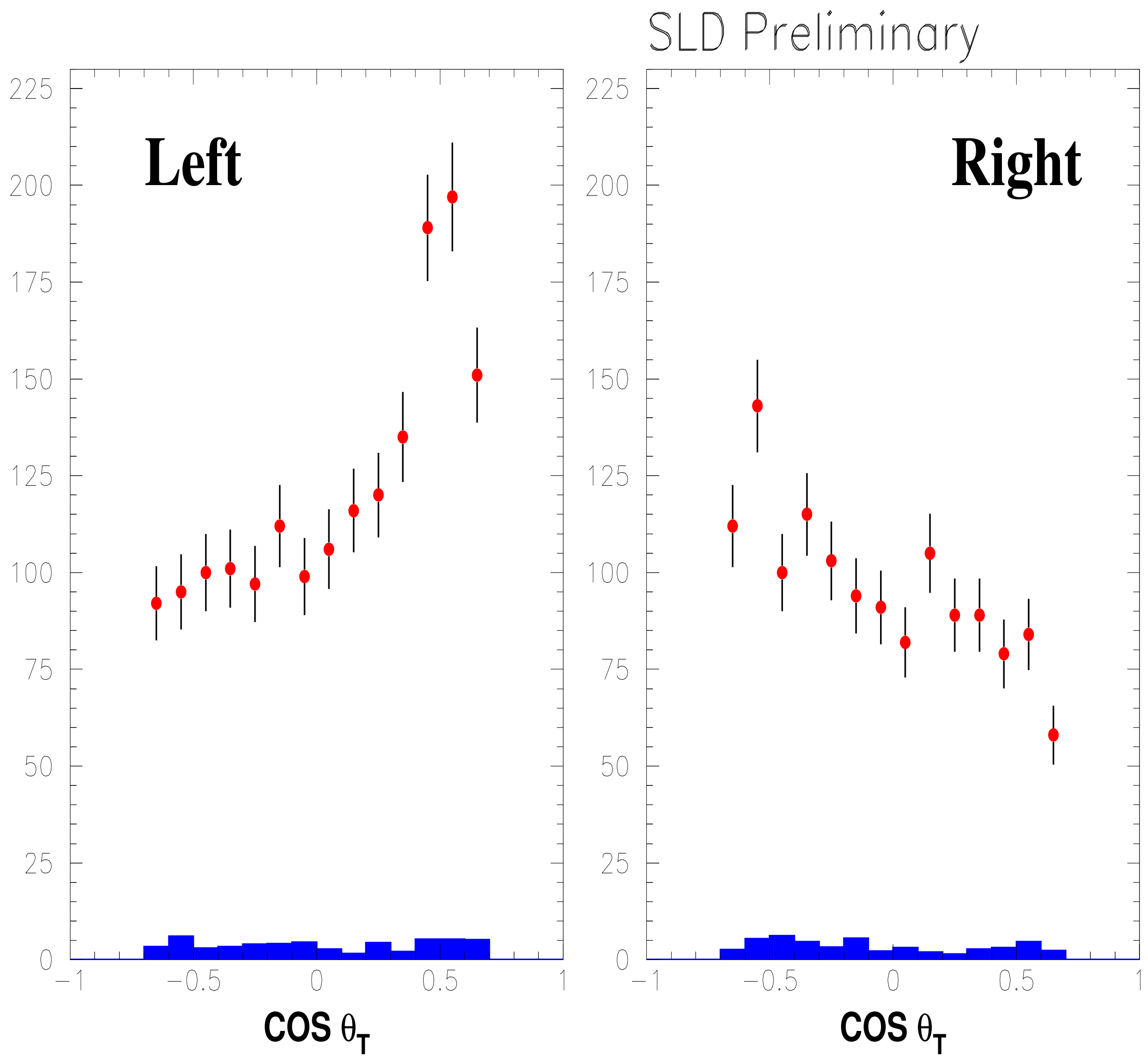

Figure 5: Distribution of the signed thrust $cos\theta$ distributions for b-tagged events with left- and right-handed electron beam polarizations. The points are for the data and the shaded histograms are MC estimated *udsc* background events.

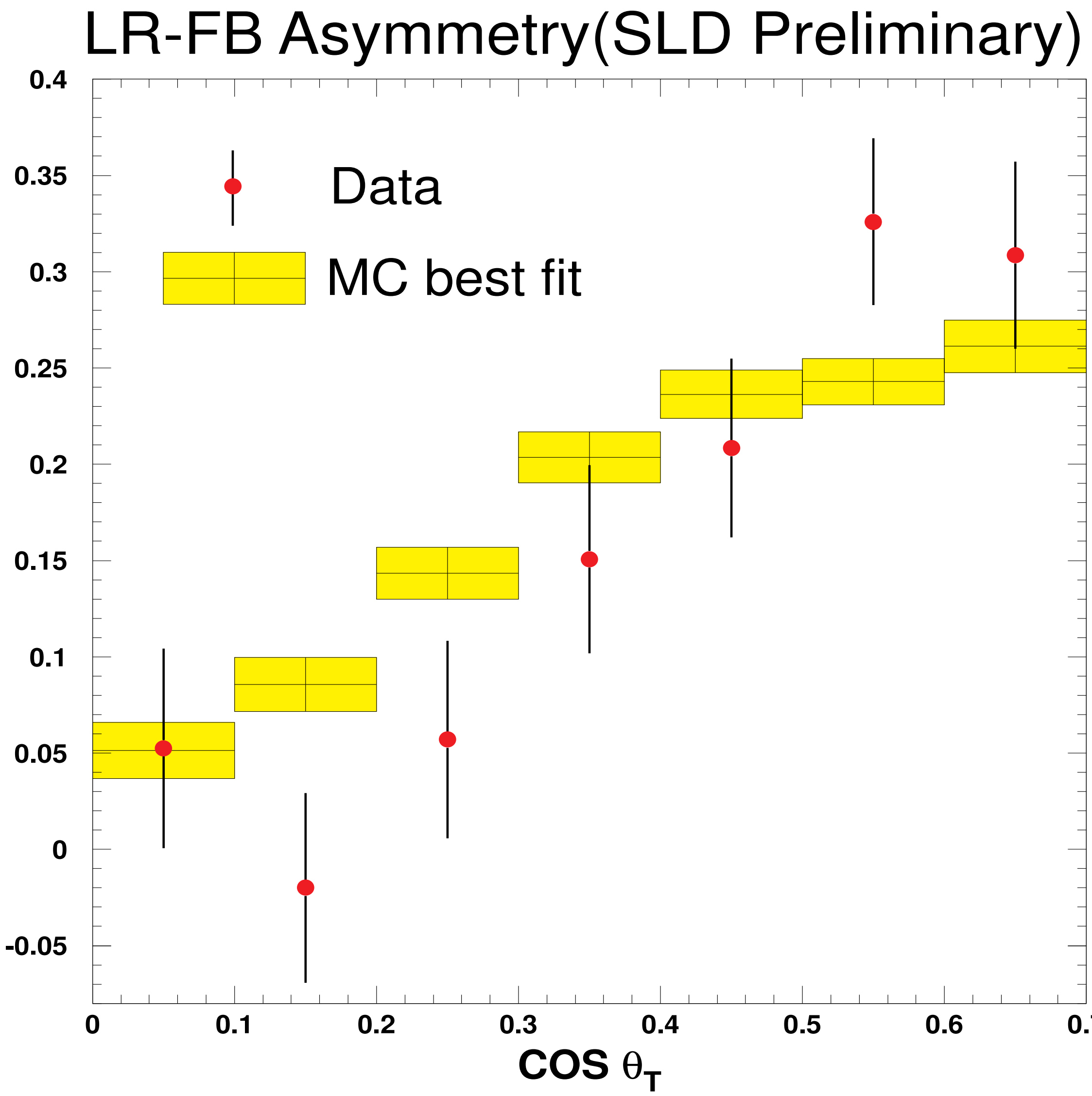

Figure 6: Left-right forward-backward for b-quarks as a function of thrust axis $cos\theta$ for background corrected data (points). The shaded boxes correspond to the best fit MC, where the vertical size of each box spans the 1 σ MC statistical errors.